Alumina-Carbon Refractory Castables Containing Calcium-Aluminate Coatings on Graphite

R. Halder, S. Moitra, H. Acharjee, A. Chakraborty, S. Mukhopadhyay

The physical properties namely bulk density, apparent porosity, cold crushing strength of carbon-containing high alumina based refractory castable containing both natural and modified graphites (94 % fixed carbon) have been evaluated within the temperature region 110–1500 °C. The densification behaviour of graphite-free and graphite-containing castable matrices has been characterized too by their thermal and thermomechanical characteristics up to 1500 °C. The role of coated graphite on improved performance of the refractory ceramics was explored by thermogravimetry, X-ray diffraction, microstructure and thermal shock resistance studies. It is suggested that the hydrophilic thin film containing calcium aluminate phases encouraged graphite retention in castable matrix.

Introduction

Al_2O_3–C refractories are used in different important areas in steel making plants. However the castables containing graphite are still not being fully commercialized in a wider scale due to its low water wettability and poor oxidation resistance. The other consequence is the uncontrolled porosity and pore size distribution of the sintered body that affects the high temperature performance of the material. It is also very important to control the workability of low cement castables containing a reasonable quantity of graphite in the matrix part. The surface modification of graphite has therefore been very popular to eliminate the drawbacks mentioned above. A lot of techniques are being attempted for this target with other allied researches [1–5], of which the sol gel technique is a very attractive one [6–10]. By this method a thin intermediate hydrophilic coating is developed over graphite. By heating, it turns to a ceramic film over graphite flakes that binds the refractory oxides within the castable matrix. It not only reduces the casting water requirement but also helps to sustain graphite within the refractory for a longer period. All these features improve the performance of the castable compared to the same prepared by uncoated graphite. The authors reported the preparation of calcium aluminate coating on 97 % carbon containing graphite and its application in a fixed castable batch composition [11–13]. It is however important to change the castable formulation as well as the graphite quality to unequivocally prove the merit of the sol-gel coating on graphite.

With this aim, the main objective of this work is to study the properties and performance of a different white fused alumina (WFA) based castable as a whole along with its matrix part containing both as-received and surface-treated graphites. It includes a special emphasis on the thermal and thermomechanical characteristics of both the castable matrices as well as the relevant microstructural analysis.

Experimental

Unlike previous work carried out, two changes have been registered in this investigation. Firstly, incorporation of more fine white fused alumina (200#, i.e. around 75 µm) in this castable as an intermediate fraction between aggregate and matrix (Tab. 1). It should make the refractory more compact and may restrict the expulsion of graphite in the oxidizing atmosphere. Secondly, unlike 97 % carbon containing graphite, this work has been carried out with natural graphite containing 94 % fixed carbon with surface area 1,82 m^2/g (code: C_1). Its ash content (4,2 %) and volatile matter (1,4 %) are also different, the rest part being moisture. Surface modification of C_1 was done by a coating of calcium alumi-

Tab. 1 Batch composition of high-alumina based castable with coated and uncoated graphites

Constituent	Content [mass-%]
Aggregate	
White fused alumina (WFA)	
B.S. sieve (mesh)	
[–6+16 , –16+30, –30+60, –60+100]	59,0
Intermediate	
WFA 200 (mesh)	13,0
Matrix	
1) Microfine alumina	10,0
2) High-alumina cement	4,0
3) Graphite (94 % FC)	5,0
[coated/uncoated]	
4) Antioxidant	0,5
5) Preformed spinel	8,0
6) Microsilica	0,5
Total (Aggregate + Matrix)	100,0

R. Halder, S. Moitra, H. Acharjee, A. Chakraborty, S. Mukhopadhyay
Department of Chemical Technology
Ceramic Engin. Division
University of Calcutta
Kolkata – 700009
India

Corresponding author: *S. Mukhopadhyay*
E-mail: msunanda_cct@yahoo.co.in

Keywords: graphite, calcium aluminate, refractory castable

Tab. 2 Representative matrix compositions of high-alumina based refractory samples with/without coated or as-received graphite

Castable Matrix (Code)	Constituent ----->	Micronized Alumina [mass-%]	Microsilica [mass-%]	Preformed Spinel [mass-%]	HAC [mass-%]	Uncoated Graphite (C_1) [mass-%]	Coated Graphite (CA'-C_1) [mass-%]
C_0		45	2,5	34,5	18	–	–
C_1+		38	2	25	15	–	20
C_1–		38	2	25	15	20	–

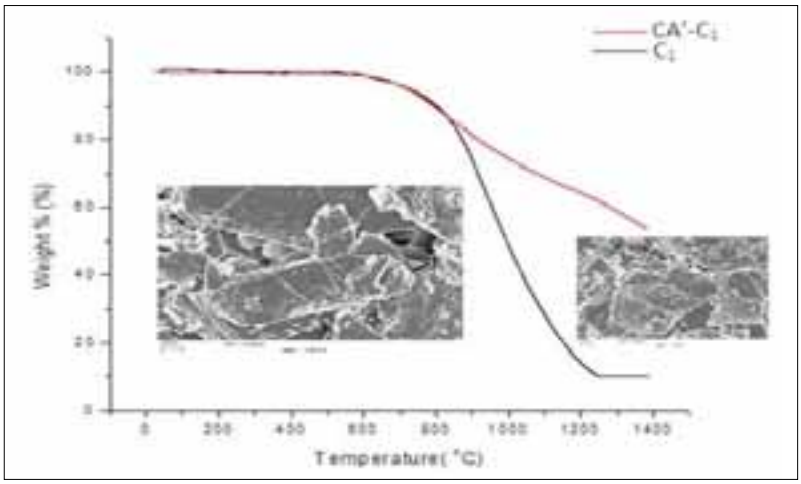

Fig. 1 Comparison of TGA patterns of coated and uncoated graphites with their inset SEM micrographs (LHS: C_1 ; RHS: CA'-C_1)

nate prepared by the sol-gel route reported previously [11–13]. Stoichiometric calcium nitrate and aluminium sec-butoxide were the main ingredients to prepare that coating. The hydrolysis and condensation reactions of the main ingredient in presence of suitable solvents at acidic pH resulted in a polymeric precursor sol. As-received flakes of C_1 were treated with this sol in presence of ultrasonication, dried and calcined (600 °C) to get the surface-treated graphite coated by calcium aluminate (code: CA'-C_1). The thermogravimetric analysis of both graphites has been carried out in air at a rate of 10 °C/min in an instrument model NETZSCH STA449F3. X-ray diffraction (XRD) phase analyses were done using a PANalytical (XPERT-PRO) instrument with Ni-filtrated CuK_α radiation.

The performance of the castable batch prepared separately by 5,0 mass-% of C_1 and CA'-C_1 (Tab. 1) have been compared and coded as C_1– and C_1+ respectively. The apparent porosity (AP), bulk density (BD) and cold crushing strength (CCS) of these two at 110, 900, 1200 and 1500 °C respectively have been determined following ASTM specifications (C20-00, C133-94 and C133-97). Preparation of castable cubes (25,4 mm^3) included dry and wet mixing for 30 min each and tamping thereafter within a certain time in moulds. Flow value and consistency of the slurry were maintained according to ASTM C 860-00 and ASTM C 230 specifications. Both C_1– and C_1+ samples have been cured in humid conditions (24 h), followed by air drying (24 h) and oven drying at 110 °C. The thermal shock resistance of the C_1– and C_1+ cubes fired previously at 1500 °C was determined in terms of percent residual strength after 5 cycles of thermal shock. Each cycle involved heating the samples at 900 °C for 5 min followed by quenching them at water at room temperature for another 5 min and then finally measuring the CCS of the samples [14].

Special attention was given separately to the matrix part of castables (below 75 µm, Tab. 2) that contained either coated or uncoated graphite. It was also compared with a matrix containing no graphite but having other microfine constituent (code: C_0). The matrices of C_1+ and C_1– corresponded to the original castable batch (Tab. 1) prepared by proportionately increasing the 27,5 % matrix part (excluding the 0,5 % antioxidant) to 100 % basis; however the C_0 matrix has been formulated by taking 22,5 % (i.e. 27,5–5) matrix constituents that did not contain any graphite fines and converting it to 100 mass-% basis (Tab. 2). The fine adjustment of other matrix constituents (microsilica, refractory cement and preformed spinel fines) in C_1+ and C_1– containing 20,0 mass-% of graphite were done by proportionately altering these to make it 100 % as shown in the Tab. 2. The differential thermal analyses (DTA) and thermogravimetry (TG) of all three castable matrices have been conducted by a Shimadzu DT-40 instrument in air at a rate of 10 °C/min to estimate the phase changes and mass loss as a function of temperature. The dimensional change under vertical load with progressively higher temperature provides an idea about the thermomechanical analysis (TMA) and densification behaviour of ceramic materials [15]. For this reason, the TMA test has been performed with those three kinds of refractory matrices up to 1500 °C in air atmosphere at a heating rate of 5 °C/min. Cylindrical bars (25 mm × 6 mm) of C_0, C_1+ and C_1– types respectively were prepared, maintaining the "ball in hand" consistency mentioned above. The test was performed by a compressive load of 100 mN in a vertical thermomechanical analyser (model TMA 402F3, NETZSCH/DE). The BD and AP of Co, C_1+ and C_1– samples heat treated at 1400 and 1500 °C respectively had been measured to verify the extent of sintering in them. Finally, the scanning electron microscope (SEM) study of some selected samples has been carried out by the instrument JEOL JSM 6700 F model.

Results and discussion

It has been reported that sol-gel route produces calcium-doped γ-alumina at 600 °C that progressively crystallizes to calcium aluminate at around 930 °C [10–13, 16–19]. The TGA loss in C_1 and CA'-C_1 shows (Fig. 1) that the rate of fall due to oxidation loss is much steeper in uncoated graphite that

almost burns out nearby 1200 °C. However the rate of fall is gradual in coated graphite and requires much higher temperature for complete oxidation. The corresponding micrograph observed in as-received graphite (LHS inset) contained a little bit of (clayey) impurities associated with it. In contrast the microstructure (inset, RHS) in the TGA plot of coated graphite shows some additional extraneous phases which are the calcined relicts of sol gel coating over the graphite flakes. These are rich in Ca-doped γ-Al_2O_3 and prevent untimely oxidation of graphite underneath. After the coating formation the main graphite peak intensity corresponding to the (002) reflection plane in C_1 has been reduced in CA'-C_1 (Fig. 2). As the coating of Ca-doped γ-Al_2O_3 spreads over the graphite surface sporadically, there has been a reduction too of clayey peaks coming from impurity associated with natural minerals. The content of clayey impurities e.g. kaolinite associated with the graphite used in this work are different from that observed in 97 % carbon containing graphite reported in last works [11–13]. The other peaks of graphite are also reduced in coated graphite for the same reason.

It is known that γ-Al_2O_3 is Lewis acidic and imparts hydrophilicity. Due to presence of this particular phase over coated graphite, the water consumption during casting of C_1+ and C_1– castable has been found to be 8,0 and 11,0 % respectively. The hydrophilic coating of doped γ-Al_2O_3over 94 % carbon containing graphite thus performs in the similar manner as was observed in 97 %. Fig. 3 shows the comparison of AP, BD and CCS properties of C_1+ and C_1– castables respectively and confirms that the former possesses much better physical characteristics. The castable batch contained 4,0 mass-% of high alumina cement, however a huge amount of casting water (11,0 %) was required for C_1– castable as usually required for conventional castables. Although the mineralogical and chemical compositions are the same in C_1+ and C_1– batches, significant changes in physical properties were thus obvious between these two in relation to firing temperatures. During hydration of cement CAH_{10}, C_2AH_8, C_3AH_6 and AH_3 phases (C = CaO, A = Al_2O_3 and H = H_2O) are generated in castable.s On heating beyond 900 °C, these hydrated compounds converts to CA and CA_2 etc. after complete dewatering. Thereafter, densification starts to reduce AP and improves CCS values within 1200–1500 °C. Although it was attempted to make a more compact castable by WFA fines (75 µm), yet it has been observed that AP increases in the C_1– castable as usual throughout 110–1500 °C due to unprotected graphite; but the sol-gel coating noticeably improved the performance of C_1+ castable.

Resistance to thermal shock or spalling is an important property desirable for graph-

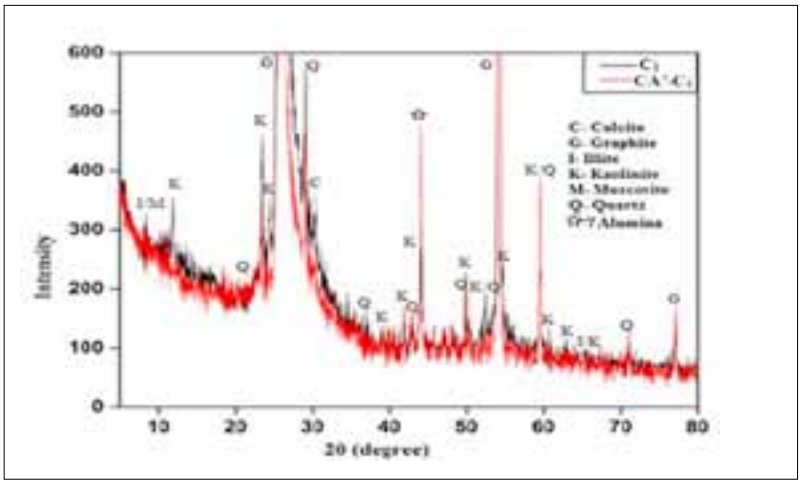

Fig. 2 Combined XRD plots of coated and uncoated graphites

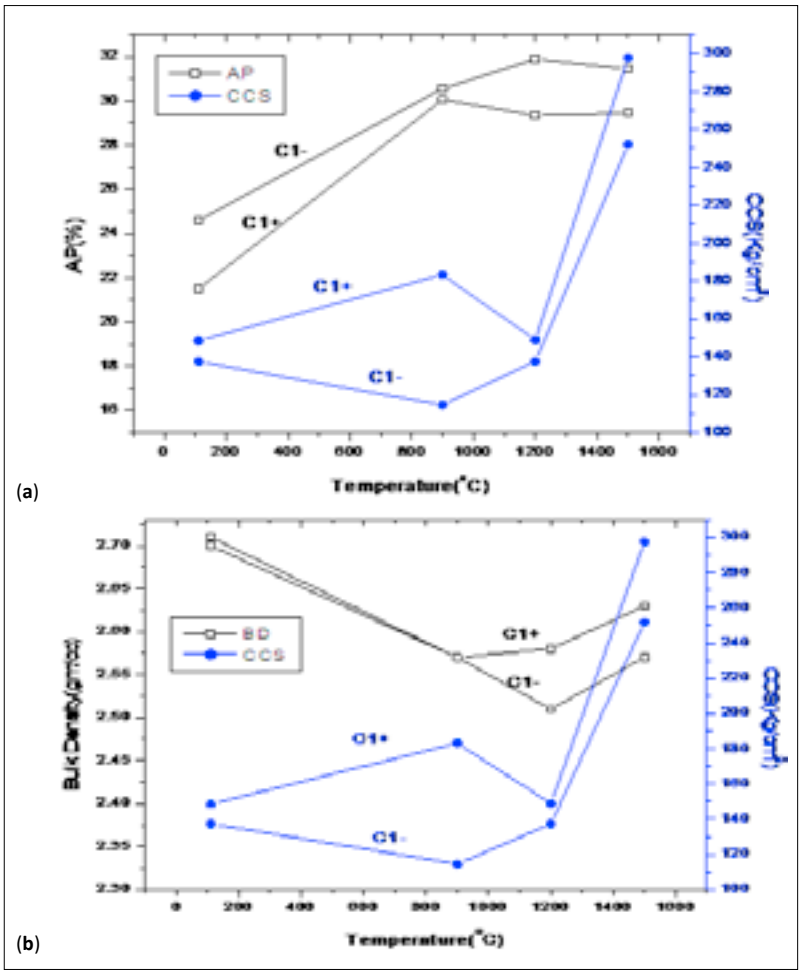

Fig. 3 Comparison of variation in physical properties of C_1+ and C_1– castables respectively with increasing temperatures: (a) AP vs. CCS plot, (b) BD vs. CCS plot

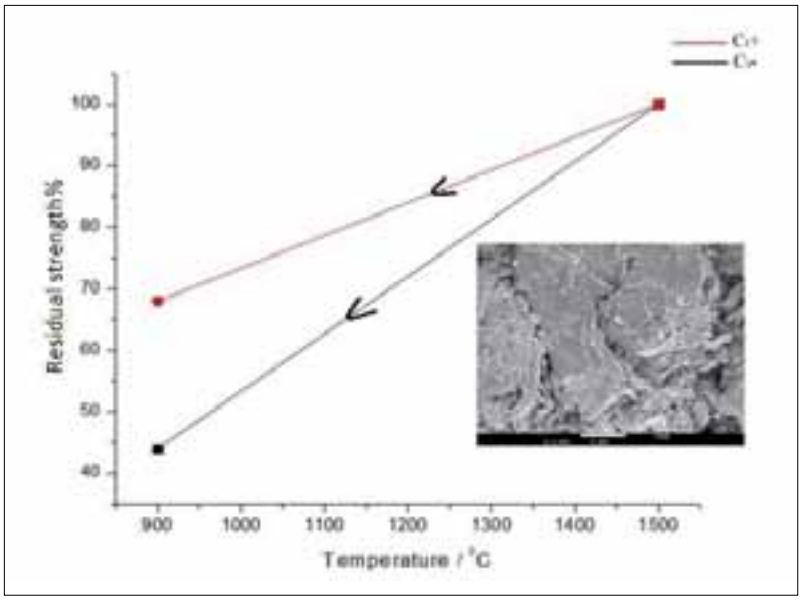

Fig. 4 Comparison of thermal shock resistance of C_1+ and C_1– castables respectively with the inset SEM micrograph of the 1500 °C fired C_1+ sample

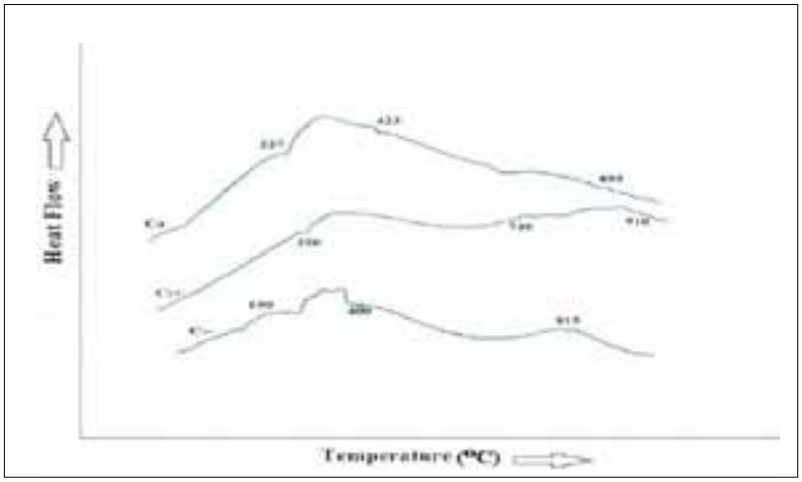

Fig. 5 Comparison of DTA traces Co, C_1+ and C_1– matrices respectively

ite containing refractory castables. Due to low thermal expansion and higher thermal conductivity, the thermal shock resistance of graphite containing castables are much appreciated. In this study (Fig. 4) it was found that residual strength of C_1+ castable is much higher (68 %) than the uncoated one (44 %). This is corroborated by the inset SEM micrograph of fired C_1+ sample that reveals a well-densified matrix having a continuous texture with retained graphite flakes. By this way, the pre-exfoliated and flexible nanosheets of graphite toughen the C_1+ castable matrix. Unlike uncoated graphite (C_1), the thin calcium aluminate coating prevents the debonding of graphite from the refractory.

Tab. 3 Comparison of AP and BD of C_1+ and C_1– matrices respectively at elevated temperatures

Sample	Moisture [%]	1400 °C		1500 °C	
		AP	BD	AP	BD
C_1+	24,3	46	1,85	52,50	1,70
C_1–	29,1	52	1,67	53,0	1,65

DTA comparison (Fig. 5) of C_1+ and C_1– matrices respectively (Tab. 2) also confirms that graphite oxidation is more conspicuous and starts earlier in C_1– nearby 800 °C due to lack of coating. It also indicates the sustainability of coated graphite in the C_1+ castable matrix that assists to improve the spalling resistance reported above (Fig. 4). Peaks of C_0 are due to the dehydration of AH_3 gel and cementitious compounds that continues up to above 400 °C. The cement-bonded matrix also corroborates formation of transient $C_{12}A_7$ phase nearby 700 °C whereas crystallization of CA phase occurs at around 900 °C. The TGA losses of the matrices of C_0, C_1+ and C_1– have been found to be 12,9, 30,5 and 39,0 % respectively. It again confirms the expulsion of more graphite and water from the C_1– matrix. As C_0 contains no graphite, its TG loss is the least among the three.

The better sinterability and improved thermomechanical pattern of C_1+ matrix compared with C_1– matrix can be understood when the TMA traces of C_1+, C_1– (and C_0) matrices respectively are compared (Fig. 6). The overall patterns of these three are almost similar up to 1100 °C as reported [15], although C_0 matrix not containing any graphite is much denser. Therefore, early shrinkage and densification is most prominent in C_0, which is complete around 1400 °C, but C_1+ and C_1– matrices respectively exhibit further densification. The maximum rate of shrinkage is observed in C_1+ sample at the tip of the lower most curve. However, C_1– sample containing more porosity due to graphite expulsion shows lesser densification by solid state diffusion via grain to grain attachment. As a consequence, the sintered BD of C_1+, C_1– and C_0 at 1400 °C are 1,85, 1,67 and 2,3 g/cm^3 respectively, whereas the respective AP values are 46, 52 and 31 % respectively (Tab. 3). The difference in water consumption of C_1+, C_1– is also another reason for such difference in BD and AP. It is also known, that in high-alumina based castable CA_6 phase (hibonite, i.e. calcium hexa-aluminate) appears above 1400 °C and increases with further increase in temperature due to the reaction between micronized alumina with CA/CA_2 phases. This hibonite formation is associated with significant volume expansion [20]. As in this work only the matrix parts have been separately considered for all

three samples, the volume expansion is reasonably high which affected the shrinkage due to sintering. Consequently, the rate of expansion (TMA) beyond 1400 °C increases in the upward direction (Fig. 6, inset). Consequently it results in a decrease in BD and increase in AP in all three samples. As such the sintered BD values of C_1+, C_1– and C_0 at 1500 °C are 1,70, 1,65 and 2,08 g/cm^3 respectively, whereas the respective AP values are 52,5, 53 and 41 % respectively. The water requirement during casting of C_1+, C_1– and C_0 matrices respectively are 24,3, 29,1 and 23,8 % respectively. From Tab. 3 it is clear that AP of coated graphite containing matrix is less than uncoated one both in 1400 and 1500 °C respectively. The C_0 matrix having no graphite is inherently denser than the other two. While comparing the AP and BD of matrices of graphite-containing castables, it is also observed that at 1500 °C, BD and AP of C_1+ deteriorate more than C_1–. Beyond 1400 °C, the volume expansion due to hibonite formation is more extensive in both of them. The authors identify the porosity difference between the two as the root cause. As the porosity in C_1– at 1400 °C is already much higher the volume expansion due to evolution of hibonite is well accommodated inside that matrix. Oppositely, the C_1+ matrix being denser at 1400 °C, fails to provide additional spaces for hibonite formation. Thus cracks and pores due to stress generation arise at 1500 °C to hinder its performance that has been displayed in Fig. 7 (inset).

The microstructure and phase evolution in the C_1+ matrix fired at 1500 °C in this regard should be highlighted (Fig. 7). The XRD pattern of C_1+ matrix shows that besides the expected phases like corundum and calcium aluminate, the strong peaks of graphite are prominently present in the matrix even after severe heat treatment. Graphite oxidation has been restricted obviously due to the calcium aluminate coating. The XRD plot also indicates the evolution of two other phases, namely silicon carbide and silicon oxide nitride the reason for which had already been elucidated previously [10–13]. It confirms again that the antioxidising characteristics are maintained within the C_1+ matrix even at 1500 °C. These phases with high aspect ratio reinforce the structure, improve the oxidation resistance and mechanical properties of the refractory. Plenty of hibonite phase and associated cracks are also visible in the micrograph inset due to the reason discussed above.

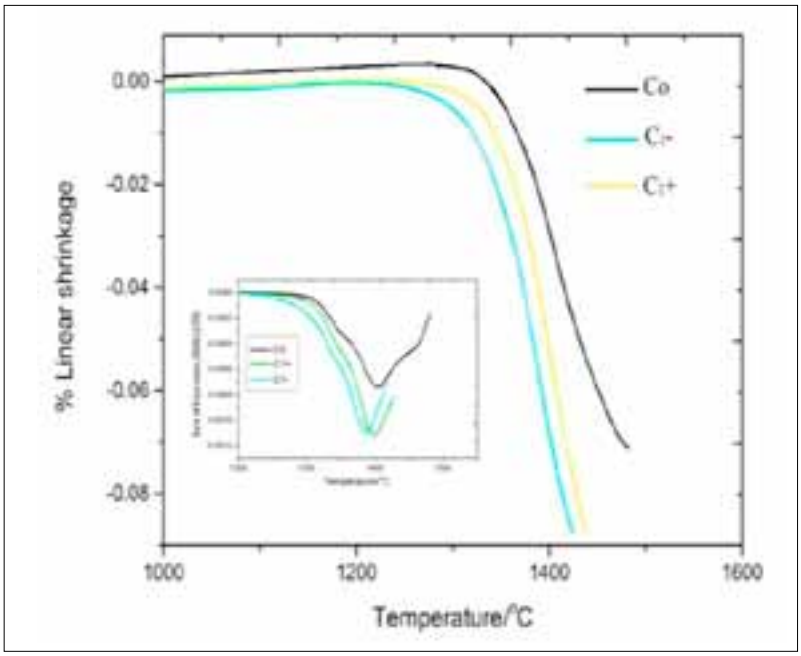

Fig. 6 Comparison of TMA patterns C_0, C_1+ and C_1– matrices respectively: linear shrinkage vs. temperature plot with the inset rate of expansion vs. temperature

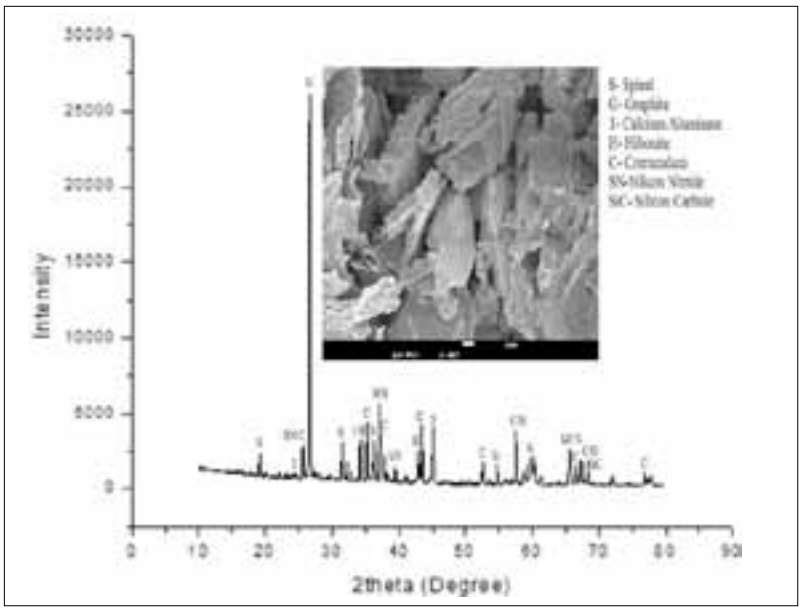

Fig. 7 XRD plot of the C_1+ matrix fired at 1500 °C with inset SEM micrograph

Conclusions

From this work done at laboratory scale, a positive indication is realised once again in favour of sol-gel coated graphite. The sinterability and other characteristics (e.g. oxidation resistance, spalling resistance) of a high-alumina based castable having surface treated graphite had been reasonably improved in comparison with that containing as-received graphite. Both the matrix and the castable as a whole consumed less water due to the hydrophilic coating of calcium-aluminate precursor. Consequently, the less porous castable bonded with coated graphite and other constituents helped to sustain carbon/graphite inside the monolithic refractory for a longer period at aggressive atmosphere.

References :

[1] Stein, V.; Aneziris, C.G.: Low carbon carbon-bonded alumina refractories for structural components in steel technology. J. Ceram. Sci.Technol. **5** (2014) [2] 115–124

[2] Lee, W.E.; Zhang, S.: Improving the water-wettability and oxidation resistance of graphite using Al_2O_3/SiO_2 sol-gel coatings. J. Europ. Ceram. Soc. **23** (2003) 1215–1221

[3] Zhang, S.; Liu, X.: Low temperature preparation of titanium carbide coatings on graphite flakes from molten salts. J. Amer. Ceram. Soc. **91** (2008) 667–670

[4] Rigaud, M.; et al.: Mechanical properties up to 1100 °C of Al_2O_3-MgO extended graphite pellet castables reinforced with steels. Ceram. Int. **35** (2009) 359–362

[5] Saberi, A.; et al.: Improving the quantity of nanocrystalline $MgAl_2O_4$ spinel coating on graphite by a prior oxidation reaction on the graphite surface. J. Europ. Ceram. Soc. **28** (2008) 2011–2017

[6] Yilmaz, S.; et al.: Synthesis and characterization of boehmitic alumina coated graphite by sol-gel method. Ceram. Int. **35** (2009) [5] 2029–2034

[7] Mukhopadhyay, S.; et al.: Spinel-coated graphite for carbon containing refractory castables. J. Amer. Ceram. Soc. **92** (2009) [8] 1895–1900

[8] Mukhopadhyay, S.: Nanoscale calcium aluminate coated graphite for improved performance of alumina based monolithic refractory composite. Mater. Res. Bull. **48** (2013) 2583–2588

[9] Mukhopadhyay, S.: Improved sol-gel spinel ($MgAl_2O_4$) coatings on graphite for application in carbon containing high alumina castables. J. Sol-Gel Sci. Technol. **56** (2010) 66–74

[10] Dutta, S.; et al.: Significant improvement of refractoriness of Al_2O_3–C castables containing calcium aluminate nano-coatings on graphite. Ceram. Int. **40** (2014) 4407–4414

[11] Mukhopadhyay, S.; et al.: In depth studies on cementitious nanocoatings on graphite for its contribution in corrosion resistance of alumina based refractory composite. Ceram. Int. **41** (2015) 11999–12010

[12] Mukhopadhyay, S.; Dutta, S.: Comparison of solid state and sol-gel derived calcium aluminate coated graphite and characterization of prepared refractory composite. Ceram. Int. **38** (2012) 4997–5006

[13] Mukhopadhyay, S.; Das, G.; Biswas, I.: Nanostructured cementitious sol gel coating on graphite for application in monolithic refractory composites. Ceram. Int. **38** (2012) 1717–1724

[14] Goodrich, H.R.: Spalling and loss of compressive strength of firebrick. J. Amer. Ceram. Soc. **10** (1927) 784–794

[15] Mukhopadhyay, S.; et al.: Thermal and thermomechanical characteristics of monolithic refractory composite matrix containing surface-modified graphite. Ceram. Int. **42** (2016) 6015–6024

[16] Goktas, A.A.; Weinberg, M.C.: Preparation and crystallization of sol-gel calcia-alumina compositions. J. Amer. Ceram. Soc. **74** (1991) [5] 1066–1070

[17] Uberoi, M.; Risbud, S.S.: Processing of amorphous calcium aluminate powders at <900 °C. J. Amer. Ceram. Soc. **73** (1990) [6] 1768–1770

[18] Douy, A.; Gervais, M.: Crystallisation of amorphous precursors in the calcia-alumina system: A differential scanning calorimetry study. J. Amer. Ceram. Soc. **83** (2000) 70–76

[19] Gulgun, M.A.; et al.: Chemical synthesis and characterization of calcium aluminate powders. J. Amer. Ceram. Soc. **77** (1994) 531–539

[20] Simonin, F.; et al.: Thermomechanical behavior of high-alumina refractory castables with synthetic spinel additions. J. Amer. Ceram. Soc. **83** (2000) [10] 2481–90